

Nonlinearities in modified gravity cosmology I: signatures of modified gravity in the nonlinear matter power spectrum

Weiguang Cui^{1,*}, Pengjie Zhang^{1,†} and Xiaohu Yang^{1,‡}

¹*Key Laboratory for Research in Galaxies and Cosmology, Shanghai Astronomical Observatory, the Partner Group of MPA, Nandan Road 80, Shanghai, 200030, China*

A large fraction of cosmological information on dark energy and gravity is encoded in the nonlinear regime. Precision cosmology thus requires precision modeling of nonlinearities in general dark energy and modified gravity models. We modify the Gadget-2 code and run a series of N-body simulations on modified gravity cosmology to study the nonlinearities. The modified gravity model that we investigate in the present paper is characterized by a single parameter ζ , which determines the enhancement of particle acceleration with respect to general relativity (GR), given the identical mass distribution ($\zeta = 1$ in GR). The first nonlinear statistics we investigate is the nonlinear matter power spectrum at $k \lesssim 3h/\text{Mpc}$, which is the relevant range for robust weak lensing power spectrum modeling at $\ell \lesssim 2000$. In this study, we focus on the relative difference in the nonlinear power spectra at corresponding redshifts where different gravity models have the same linear power spectra. This particular statistics highlights the imprint of modified gravity in the nonlinear regime and the importance of including the nonlinear regime in testing GR. By design, it is less susceptible to the sample variance and numerical artifacts. We adopt a mass assignment method based on wavelet to improve the power spectrum measurement. We run a series of tests to determine the suitable simulation specifications (particle number, box size and initial redshift). We find that, the nonlinear power spectra can differ by $\sim 30\%$ for 10% deviation from GR ($|\zeta - 1| = 0.1$) where the rms density fluctuations reach 10. This large difference, on one hand, shows the richness of information on gravity in the corresponding scales, and on the other hand, invalidates simple extrapolations of some existing fitting formulae to modified gravity cosmology.

PACS numbers: 98.65.Dx, 95.36.+x, 04.50.+h

I. INTRODUCTION

One of the biggest challenges of modern cosmology and physics is the existence of the *dark* universe. Assuming the validity of general relativity (GR), cosmological observations lead to the discovery of dark matter and dark energy, which account for $\sim 96\%$ of the total matter and energy budget of the Universe (e.g. [1]). However, since we do not have independent tests of GR at relevant scales, the same set of observations could imply another possibility, the failure of general relativity at galactic and cosmological scales. This possibility, which serves as an alternative to dark matter/dark energy, has become an area of active research. Discriminating between the dark matter/dark energy and modified gravity (MG) models, testing GR at cosmological scales and probing dark matter and dark energy through cosmological observations, are thus an entangled task, of crucial importance for both cosmology and physics.

Challenges exist in both the observation side and theory side. Although there are numerous and potentially powerful observations suitable for this task [2, 3], their precision measurements are challenging. On the other hand, much of the cosmological information is encoded in the nonlinear regime. Modeling the nonlinearities to

the required $\sim 1\%$ accuracy is challenging too, even for the simplest case, the standard ΛCDM cosmology with only gravitational interaction (e.g. [4–7]). Cosmologies based on dynamical dark energy or MG are facing similar requirements. References [6–11] have performed N-body simulations for dynamical and coupled dark energy models [12].

Comparing to the dark matter/dark energy cosmology, understanding the evolution of the Universe in MG models is often more difficult, due to the intrinsically nonlinear feature of gravity in these models or the existence of extra dynamical fields. Despite these difficulties, the expansion history of the Universe and the structure growth to the first order have been robustly understood for many of the MG models such as TeVeS [13, 14], DGP (short for Dvali, Gabadadze and Porrati) [15, 16] and the $f(R)$ gravity [17–21]. People have also achieved success in understanding the nonlinear evolution through analytical and semianalytical methods (e.g. [22–25]). Recently, self-consistent gravity solvers for $f(R)$ [26–29] and DGP gravity [30] models have been developed and led to significantly improved understanding of the nonlinear evolution. Simulations with extra scalar fields and interaction with dark matter have also been performed (e.g. [31]).

Since deviations from GR in general lead to nonlinear differential equations of gravity, in principle we have to develop the suitable N-body codes for each viable MG model and run the corresponding simulations. However, since we do not have the final theory of gravity based on the first principles, there are in principle infinite MG

*Electronic address: wgcui@shao.ac.cn

†Electronic address: pjzhang@shao.ac.cn

‡Electronic address: xhyang@shao.ac.cn

models to be investigated. One possibility to circumvent this problem is to choose a suitable parameterization for the MG models and run a finite number of simulations to sample the relevant parameter space. We are then able to interpolate/extrapolate the simulation results to explore the whole relevant parameter space.

The statistics we focus on is the matter power spectrum. It determines the lensing power spectrum and is also highly relevant to the 2D galaxy clustering, both will be measured to high precision by ongoing and planned imaging surveys, such as DES, LSST, JDEM/SNAP, Euclid/DUNE, and KDUSt. As we will show later, the density evolution is determined by a single parameter of gravity, ζ , which quantifies the ability of mass concentration to distort the space-time metric. In principle, ζ can be both scale, time, and environmental dependence. Comprehensive investigation on general ζ is beyond the scope of the current paper. Instead, we will adopt a highly simplified form of ζ and run a series of N-body simulations to quantify the nonlinear evolution of the Universe.

As shown in Heitmann et al. 2008, (hereafter H08, [5]), however, to run simulations and model nonlinear matter power spectrum to 1% accuracy to $k \sim 1h\text{Mpc}$ is very challenging, requiring Gpc or larger simulation box size, 1024^3 or more particles, and beyond. Being aware of these difficulties and limited computation resource, we take a modest goal, to quantify the *influence* of MG on the nonlinear matter power spectrum with respect to the standard ΛCDM to $\sim 1\%$ accuracy. Namely, the statistics that we will focus on is the *relative difference* between the nonlinear matter power spectra in the given MG model and in ΛCDM . We will choose the right redshifts of simulation output such that the linear matter power spectra in the given MG models are equal to the ones in the corresponding ΛCDM . This particular statistics has a number of attractive features. First, it isolates and highlights the role of MG in nonlinear evolution. Second, it reduces much of the numerical artifacts by taking ratios. Similar tricks have been adopted in many previous simulations (e.g. [8–10]). Third, it can improve the efficiency to understand nonlinearities in MG models, which can now be reduced to two separate ingredients: the nonlinear evolution in ΛCDM and the relative difference between MG models ΛCDM .

The current paper only analyzes a very limited set of simulations. Nonetheless, it robustly show that, even after scaling out the difference in the linear evolution, gravity still leaves significant features in the nonlinear power spectrum. In subsequent studies, we will run simulations covering larger parameter space to better understand these features and hopefully develop a general fitting formula. Furthermore, we will study the peculiar velocity power spectrum and the redshift distortion (3D galaxy clustering), based on these simulations. The ongoing spectroscopic redshift surveys like BOSS, LAMOST and WiggleZ, and planned spectroscopic redshift surveys like BigBOSS, JDEM/ADEPT, Euclid/SPACE and SKA

are able to measure these statistics to unprecedented accuracy. We will also investigate the halo statistics, one of the key scientific goals for galaxy and cluster surveys.

This paper is organized as follows. In Sec. II, we present the MG parameterization adopted for the simulations, the precision requirements and the code specifications. In Sec. III, we test the accuracy of the simulations. We present major simulation results in Sec. IV, discussion in Sec. V and more results in the Appendix.

II. THE SIMULATION LAYOUT

A. The ζ parameterization on modified gravity

There are several existing parameterizations and general guidances on modified gravity [3, 22, 32–38]. What we adopt in this paper is the ζ parameterization. It is a condensed version of the $G_{\text{eff}}\text{-}\eta$ parametrization [3, 36], which quantifies two key aspects of gravity.

To understand this point, we begin with the structure formation in GR, for which the central issue is to determine the particle acceleration given the mass distribution. The scalar perturbation of the space-time metric is described by two potentials, $ds^2 = -(1+2\psi)dt^2 + a^2(1+2\phi)d\mathbf{x}^2$. The usual Poisson equation, $k^2\phi = 4\pi G a^2\delta\rho$ (in Fourier space), relates the potential ϕ to the matter distribution ρ . However, ϕ is not the potential directly responsible for the structure formation in our N-body simulations of nonrelativistic cold dark matter particles. The contribution to the particle acceleration from this potential is suppressed by a factor $(v/c)^2 \ll 1$, comparing to the contribution from the other potential ψ . Thus for the nonrelativistic cold dark matter particles that our simulations deal with, their acceleration is determined solely by ψ , $d(a\mathbf{v})/dt = i\mathbf{k}\psi$, where \mathbf{v} is the proper motion. GR predicts $\psi = -\phi$, if dark energy anisotropic stress is negligible. Now, given an initial mass distribution ρ , we obtain ϕ from the Poisson equation, with the coupling constant G . Then through the relation $\psi = -\phi$, we obtain ψ and then the acceleration. Thus given the initial positions (density) and velocities of particles, we can move particles in each simulation time step and then have a closed procedure to simulate the evolution of the Universe under gravity.

A natural parametrization of modified gravity is thus to replace the Newton's constant G by the effective Newton's constant G_{eff} and the relation $\psi = -\phi$ by $\eta \equiv -\phi/\psi$. Now, given the mass distribution, the acceleration is solely determined by the combination ζ [72],

$$\zeta(k, z) \equiv \frac{G_{\text{eff}}(k, z)/G}{\eta(k, z)}. \quad (1)$$

This is the quantity that enters into the ψ - ρ relation,

$$k^2\psi = -\zeta 4\pi G\delta\rho. \quad (2)$$

GR has the value $\zeta = 1$. Clearly, if the two universes have the identical initial conditions, identical expansion

rate and identical $\zeta(k, z)$, the statistics of the density and velocity fields would be identical [73].

Thus, instead of running a series of simulations on a 2D grid of $G_{\text{eff}}\text{-}\eta$ parameter space, we just need to run a series of simulations on a 1D grid of ζ parameter space. It significantly reduces the amount of simulations required. This is the major reason that we adopt this single parameter parametrization on modified gravity. Besides it, there are a number of attractive features of this parametrization.

First of all, many MG models, such as the DGP gravity model [16] and the $f(R)$ gravity model [18, 19] (in the linear regime), the Yukawa-like MG model and the γ -index MG model [32] fit into this parameterization. Second, such parameterization requires minimum modification in the N-body gravity solver, does not require extra computation time, and thus is suitable for fast exploration of the vast parameter space of MG models. In fact, there already exists a number of simulations on Yukawa-like gravity [39, 40]. Third, G_{eff} and η (and hence ζ), can be measured in a rather model independent manner, by combining imaging surveys and spectroscopic surveys [36, 41]. This links theories and observations directly. Furthermore, the reconstruction accuracy can be improved by including all available data and performing a multiparameter fitting [42, 43].

Clearly, this parameterization does not capture all features of MG, such as the environmental dependence of gravity, as found in $f(R)$ gravity [44] and the DGP model [45]. Nevertheless, the simulations based on this parameterization serve as an useful step toward better understanding of MG cosmology. The simulation results can be used as templates to understand more complicated MG models. A close analogy is the scale-free simulations. Although the real CDM(cold dark matter) transfer function is certainly not scale-free (power-law), these scale-free simulations do significantly improve our understanding of the nonlinear evolution of structure formation. They are helpful in developing fitting formula like that of Peacock-Dodds (hereafter PD96, [46]) and Smith et al. 2003 (hereafter halofit, [47]). We hope that similar procedure applies to the case of MG models. For example, the formalism proposed by [22] relies on the interpolation between the nonlinear power spectrum in GR and the one in MG without environmental dependence. Understanding the nonlinearities in MG models without environmental dependence thus serves as a natural step to understand nonlinearities in more complicated MG models.

Modifying existing N-body codes to incorporate the ζ parameterization is straightforward. The only modification is to change the particle acceleration \vec{a} to $\zeta \times \vec{a}$. In the simulation setup, we fix the expansion rate identical to that of the flat Λ CDM cosmology [74]. In addition, we do not aim to explore the whole space of $\zeta(k, z)$. Rather, we will focus on very special cases of ζ and postpone the general investigation for future studies. The $\zeta(k, z)$ adopted in our simulations is scale independent ($\zeta(k, z) = \zeta(z)$).

The success of CMB (cosmic microwave background) and BBN (big-bang nucleosynthesis) implies that GR is likely valid in the early Universe. For this reason, we adopt a step function in z , such that $\zeta = 1$ at $z \geq z_{\text{MG}}$ and $\zeta = \text{constant} \neq 1$ at $z < z_{\text{MG}}$. Throughout this paper, we have adopted $z_{\text{MG}} = z_i = 100$, where z_i is the initial redshift of simulations. Since we have GR valid at high redshift ($z \geq 100$), the transfer function at $z_i = 100$ adopted in the MG models is identical to that in GR. For the adopted MG parameterization, the linear density growth factor $D(k, z)$ is scale independent $D(k, z) = D(z)$. Thus the linear power spectrum for modified gravity models only differs from Λ CDM by the linear density growth factor $D(z)$. In a companion paper, we will explore MG models with other redshift dependence.

B. The precision requirements

All MG simulations begin with the identical initial condition at $z_i = 100$. Since the adopted ζ is scale independent, the linear density growth factor $D(z, \zeta)$ is scale independent, as can be seen from the equation at $z < z_{\text{MG}}$,

$$\delta_m'' + \delta_m' \left[\frac{3}{a} + \frac{H'}{H} \right] - \zeta \times \frac{3 \Omega_0 H_0^2}{2 H^2 a^3} \frac{\delta_m}{a^2} = 0. \quad (3)$$

Here, $' \equiv d/da$ and $'' = d^2/da^2$. Ω_0 is the present day matter density in unit of the critical density. H_0 and H are the present day Hubble constant and the Hubble parameter at $z = 1/a - 1$. δ_m is the linearly evolved matter over-density and $D \propto \delta_m$ is the linear density growth factor. Thus, given a redshift z_S in the standard Λ CDM, we can find the corresponding redshift z_ζ in the MG universe, such that

$$D(z_S, \zeta = 1) = D(z_\zeta, \zeta). \quad (4)$$

Here, the subscript S denotes the standard Λ CDM cosmology. Since all the simulations begin with the identical initial condition, the above relation means that,

$$P_L(k; z_S, \zeta = 1) = P_L(k; z_\zeta, \zeta).$$

Here P_L is the linear matter power spectrum. Throughout this paper, we use the subscript ‘‘L’’ for the linear statistics and the subscript ‘‘NL’’ for the nonlinear statistics.

Modifications in GR change the structure growth history. The structure grows faster in a universe with bigger ζ . The primary quantity that we want to measure through the simulations is

$$\epsilon(k; z_\zeta, \zeta) \equiv \frac{P_{\text{NL}}(k; z_\zeta, \zeta)}{P_{\text{NL}}(k; z_S, \zeta = 1)}. \quad (5)$$

$\epsilon \neq 1$ has a number of implications. (1) If the nonlinear power spectrum is completely determined by the linear one, independent of the expansion and structure growth

history and the underlying gravity, then $\epsilon = 1$. A number of fitting formulae applicable to GR have been extended to study the nonlinear evolution in MG models, based on this assumption. Thus ϵ provides a direct test on the applicability of these fitting formulae to MG models. Precision cosmology requires that, only if $|\epsilon - 1| \lesssim 10^{-2}$ in the relevant k range, may the systematical error induced by these fitting formulae be subdominant. Otherwise, significant modifications shall be made. (2) $\epsilon \neq 1$ also means that there is extra information of gravity encoded in the nonlinear matter power spectrum, which does not show up in the linear power spectrum at the same epoch. This helps to test GR at nonlinear regimes. Such information is complementary to those in the linear power spectrum at the same epoch and those in the deeply nonlinear regime where gravity reduces to GR through environmental dependence mechanisms like the chameleon mechanism and the Wainshtein mechanism [48].

Much of the cosmological information in weak lensing surveys come from the lensing power spectrum measurement at $\ell \lesssim 2000$ of source galaxies at $z_s \simeq 1$. Since the lensing kernel peaks at half way between the source and the observer, the peak contribution comes from $k \simeq \ell/[\chi(z_s)/2] \lesssim 2h/\text{Mpc}$. At $\ell = 2000$, the statistical error in the lensing power spectrum measurement can reach below 1% for the planning of wide surveys. Under the Limber approximation, the lensing angular (2D) power spectrum is linearly proportional to the 3D nonlinear matter power spectrum. Thus, to match the observation accuracy, we set a goal to model ϵ to $\sim 1\%$ accuracy at $z \sim 0.5$ and $k < 3h/\text{Mpc}$.

Since the simulations run from the identical initial condition, the cosmic variances in the resulting power spectra P_{NL} of different MG models are highly (positively) correlated. Since the simulations are run by the same code, with the same time steps, errors induced by the numerical artifacts into P_{NL} should also be highly (positively) correlated. When taking the ratio of two power spectra to evaluate ϵ , much of the errors in P_{NL} cancels. We thus expect higher accuracy in ϵ than in P_{NL} . Thus, once we control the error in P_{NL} to $\sim 1\%$ accuracy, we are likely able to measure ϵ to 1% accuracy.

We run a set of $N = 512^3$ particle N-body simulations using the GADGET-2 code, on the 32-CPU Itanium server at the Shanghai astronomical observatory. All the simulations that we use to calculate ϵ adopt $L = 300h^{-1}$ Mpc. Adopting a smaller box size allows us to go deeper into the nonlinear regime. However, a smaller box size can cause numerical artifacts, due to the missing of power at $k < 2\pi/L$, which affects the nonlinear evolution through mode coupling [5]. Another reason that we do not adopt a smaller box size is that, we plan to use the same simulations for velocity and halo statistics, which prefer a larger box size.

C. The GADGET-2 simulation specifications

We adopt a parallel GADGET-2 N-body code [49, 50] to run the simulations. With a TreePM algorithm, where only short-range forces are computed with the “tree” method while long-range forces are determined by particle mesh (PM) algorithm, GADGET-2 combines high efficiency with high resolution.

The background expansion history is fixed as the one in a flat Λ CDM cosmology with the matter density $\Omega_0 = 0.276$ and the cosmological constant $\Omega_\Lambda = 0.724$. The transfer function is fixed by the above parameters, the baryon density $\Omega_b = 0.046$ and the dimensionless Hubble constant $h = 0.703$. The amplitude of the initial fluctuations is fixed such that, if linearly evolved to $z = 0$ in the adoption of Λ CDM cosmology, the rms density fluctuation within a sphere of radius $8h^{-1}\text{Mpc}$ is $\sigma_8 = 0.811$.

We use 512^3 PM mesh grids through all the simulations. The force softening length γ depends on the mean inter particle separation, with $\gamma = 0.022L/N^{1/3}$, where L is the box size and N is the particle number. For simulations performed with 512^3 particles in the $300h^{-1}\text{Mpc}$ box, $\gamma = 12.89h^{-1}\text{kpc}$. In GADGET-2, the adaptive time step is set by $\Delta t = \sqrt{2\xi\gamma/|a|}$, where ξ controls time step accuracy and a is the acceleration. ξ is fixed at 0.5% for all the simulations. With the adopted small softening length, the number of total adaptive time steps for our Λ CDM simulation is about 4000. Fig. 13 of H08 shows that, for 3000 time steps in total, the resulting difference in the power spectra is less than 0.04%. We thus believe that, the time stepping we adopt suffices for the purpose of this paper.

III. SIMULATION TESTS

In this section, we present steps to control the robustness of simulation results. We adopt the Daubechies mass assignment method to improve the accuracy of power spectrum measurement. We run a number of tests to justify that the adopted simulation specifications (particle number, simulation box size and initial redshift) are adequate to constrain the nonlinear power spectrum out to $k = 3h\text{Mpc}^{-1}$ with $\sim 1\%$ accuracy. Finally, we show that the modified GADGET-2 code reproduces the correct linear evolution in the linear regime.

A. Calculating the matter power spectrum

Usually people use the fast Fourier transform (FFT) to calculate the matter power spectrum. This requires assigning simulation particles to uniform grids first. For commonly used mass assignment methods, the resulting power spectrum is biased by the smoothing and aliasing effects, even at scales well below the Nyquist frequency (e.g. [51]). To reach the required accuracy, we must

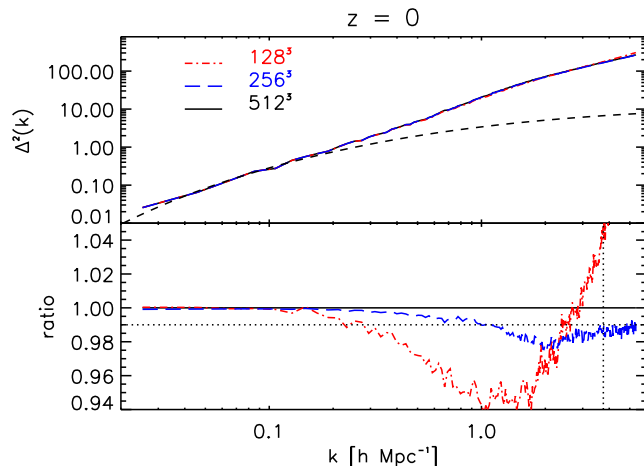


FIG. 1: The top panel shows the matter power spectra for simulations of different particle numbers. The bottom panel shows the ratios with respect to 512^3 particle simulation. All the power spectra are calculated through FFT on 512^3 meshes. The dotted vertical line shows the scale of $0.7k_{\text{Ny}}$ for our FFT power spectrum measurement. The black long dashed line is the linear power spectrum. At $z = 0$, nonlinear correction becomes significant at $k > 0.2 h \text{Mpc}^{-1}$.

correct for these biases. Reference [51] proposes an iterative method to perform such task. Alternatively, [52] adopts the Daubechies wavelet transformation for the mass assignment. The scale function of the Daubechies wavelets transform has compact top-hat like support in the Fourier space, which avoids the sampling effect and allows computationally efficient mass assignment onto grids. Using this scale function to do the mass assignment allows for robust measurement of the power spectrum to $k = 0.7k_{\text{Ny}}$ [52]. Throughout this paper, we will adopt this method to calculate the matter power spectrum.

B. Particle number

The particle number in GADGET-2 controls the mass resolution, force resolution and the time step. A larger particle number is necessary to avoid errors from discreteness effects at small scales of interest. As pointed out by Sirko [53], although simulations can probe the evolution of structures beyond the particle Nyquist frequency, $k_{\text{Ny,p}} = \pi N^{1/3}/L$, it is unclear whether or not the shot noise term beyond this frequency already in the initial condition will impact power at the wavenumbers of interest. The issue may be made moot merely by using negligible values of V/N in simulations. How many particles are required to sufficiently sample the density field and calculate the matter power spectrum robustly to $k = 3h/\text{Mpc}$? To answer this question, we run three simulations with identical initial conditions and a box size of $300 h^{-1}\text{Mpc}$, but with 128^3 , 256^3 and 512^3 particles, respectively. Fig. 1 shows the nonlinear power

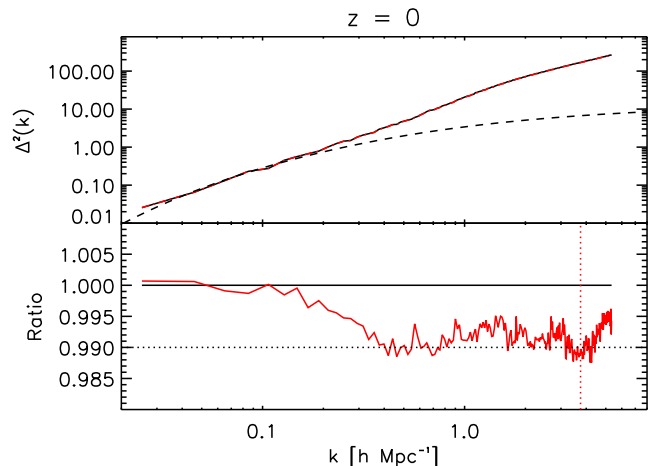


FIG. 2: The impact of initial redshift on the matter power spectrum. In the top panel, we show the power spectra of the two simulations with starting redshift $z_i = 49$ (red line) and $z_i = 100$ (the black line). The bottom panel shows the relative difference. The black horizontal dotted line shows the 1% precision requirement. The red vertical dotted line is $0.7k_{\text{Ny}}$. The same as Fig. 1, the black long dashed line shows the linear power spectrum.

spectra calculated by the Daubechies' mass assignment method. We see clearly the impact of particle number on the simulated power spectrum in the nonlinear regime. The relative difference between the 256^3 and 128^3 results at $1h/\text{Mpc} \lesssim k \lesssim 3h/\text{Mpc}$ is $\sim 4\%$, implying a minimum error of 4% in the 128^3 particle simulation, due to the resolution limitation. But the relative difference reduces to below 1-2% between the 512^3 and 256^3 ones, showing that the resolution induced error in the 256^3 particle simulation is reduced significantly. This trend of convergence implies that the resolution induced error in the 512^3 simulation is likely below $\sim 1\%$. We then speculate that, if the Daubechies' mass assignment method was adopted, nonlinear power spectrum in the 512^3 particle simulation can attain $O(1\%)$ accuracy out to $k \sim 3 h \text{Mpc}^{-1}$. To robustly test it, higher resolution simulations (e.g. ones with 1024^3 particles or more) are required. This test shall be performed in future works.

C. Initial redshift

Testing the effect of changing the starting redshift in simulations is also important. Since the initial condition is generated under the Zel'dovich approximation [54], the initial redshift z_i can not be too low, otherwise higher order corrections can be non-negligible. However, it is not automatically the case that higher z_i is better, because numerical errors (most obviously suppression of power by limited force resolution) have more time to accumulate in that case [8]. Our initial redshift tests are started at $z_i = 49$ and $z_i = 100$ respectively, both with 512^3 par-

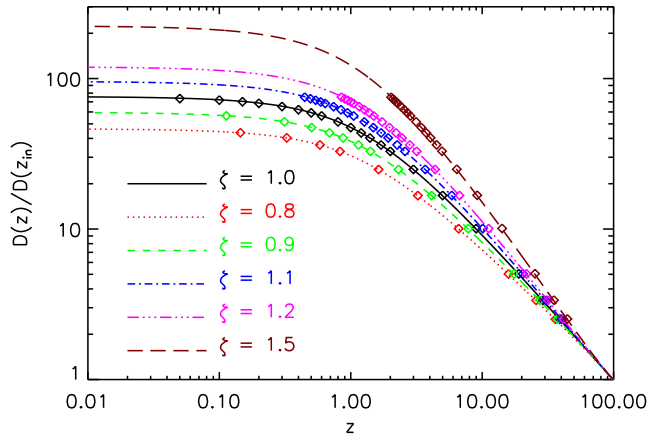


FIG. 3: The linear density growth, normalized at $z = z_i = 100$. The squares are obtained from the power spectra at $k = 0.025 h\text{Mpc}^{-1}$ in the simulations. The corresponding redshifts are shown in Table I. The different colored and style lines are the theoretical predictions. The agreement between the simulated results and theoretical predictions justifies our modified GADGET-2 code for MG models.

ticles and a $300 h^{-1}\text{Mpc}$ box size. Fig. 2 compares the two power spectra at redshift $z = 0$. The agreement is better than 1%. We then justify the choice of $z_i = 100$.

D. Simulation box size

As discussed by H08 and [8], box size affects nonlinear power spectrum mainly through two effects. One is the sample variance. Smaller box size simulation suffers larger statistic fluctuations due to fewer independent modes. Our results are relatively insensitive to this sample variance, because we take the ratio of the power spectra, which share more or less the same cosmic variance, thus the ratio will cancel much of this sample variance. The other is systematic errors induced by missing large-scale modes, which contribute to the tidal force. Reference [8] (see Fig. 9 of [8]) shows that the systematic error is substantially small ($< 1\%$ at $z = 0$) even in box size $L = 110 h^{-1}\text{Mpc}$ out to $k = 10 h\text{Mpc}^{-1}$. We thus think that the $300 h^{-1}\text{Mpc}$ box size is suitable. For the adopted box size, the largest available mode lies in the linear regime even at $z = 0$, allowing us to test the simulation result against the linear evolution to check the modified GADGET-2 code.

Based on the above tests, we justify that, with 512^3 particles, a $300 h^{-1}\text{Mpc}$ box size and initial redshift $z_i = 100$, N-body simulation based on GADGET-2 can help us reliably probe the matter power spectrum to $k = 3 h\text{Mpc}^{-1}$. The primary statistics that we investigate in this paper, ϵ , namely the ratio of power spectra of MG models and ΛCDM , can reach unity to an accuracy of 1%. As we will find later, in MG models, even

for those with moderate deviation from GR (e.g. 10% deviation), ϵ can deviate from unity to $O(0.1)$, an order of magnitude larger than the simulation error. We thus are confident that the resulting ϵ is robust.

$\zeta(z < 100)$	0.8	0.9	1.0	1.1	1.2	1.5
			ΛCDM			
Redshift	36.08	37.60	39.00	40.27	41.49	44.52
	25.74	27.45	29.00	30.41	31.73	35.17
	15.86	17.49	19.00	20.42	21.74	25.24
	6.623	7.830	9.000	10.11	11.20	14.18
	3.238	4.125	5.000	5.870	6.723	9.167
	1.628	2.311	3.000	3.689	4.383	6.412
	0.828	1.414	2.000	2.586	3.179	4.949
	0.583	1.145	1.700	2.255	2.816	4.502
	0.326	0.874	1.400	1.925	2.453	4.049
	0.145	0.689	1.200	1.703	2.210	3.745
		0.504	1.000	1.485	1.972	3.442
		0.313	0.800	1.269	1.732	3.142
		0.113	0.600	1.053	1.500	2.847
		0.00719	0.500	0.947	1.383	2.700
		N/A	0.400	0.843	1.271	2.554
		N/A	0.300	0.741	1.160	2.415
	N/A	0.200	0.639	1.053	2.281	
	N/A	0.150	0.591	1.002	2.216	
	N/A	0.100	0.541	0.951	2.152	
	N/A	0.050	0.494	0.901	2.090	
	N/A	0.000	0.447	0.850	2.029	

TABLE I: The output redshifts for the simulation of each ζ . The baseline redshifts z_S are that of $\zeta = 1$ (ΛCDM). The corresponding redshifts z_ζ of $\zeta \neq 1$ are set up by $D(z_S, \zeta = 1) = D(z_\zeta, \zeta)$.

E. Checking Modified GADGET-2

For the MG parameterization we adopt Eq. 2, we only need to do a minimal modification to the GADGET-2 code [50]. The original code calculates the gravitational potential in GR. Multiplying it by a factor ζ , we obtain the potential ψ in the MG models, which determines the acceleration of nonrelativistic particles. In GADGET-2, because the TreePM algorithm is adopted, the gravitational potential is explicitly split into a long-range part and a short-range part. We need to multiply both by the same factor ζ .

We test the modified GADGET-2 code by comparing the simulated linear growth and the theoretically calculated one. In the linear regime, the matter power spectrum $P(k, z) \propto D^2(z)$. The scale $k = 0.025 h\text{Mpc}^{-1}$ is in the linear regime through all output redshifts, so we calculate the power spectrum at this scale and compare it to the theoretical prediction, given by Eq. 3. Fig. 3 shows the comparisons. The good agreement indicates that our modified GADGET-2 is correct.

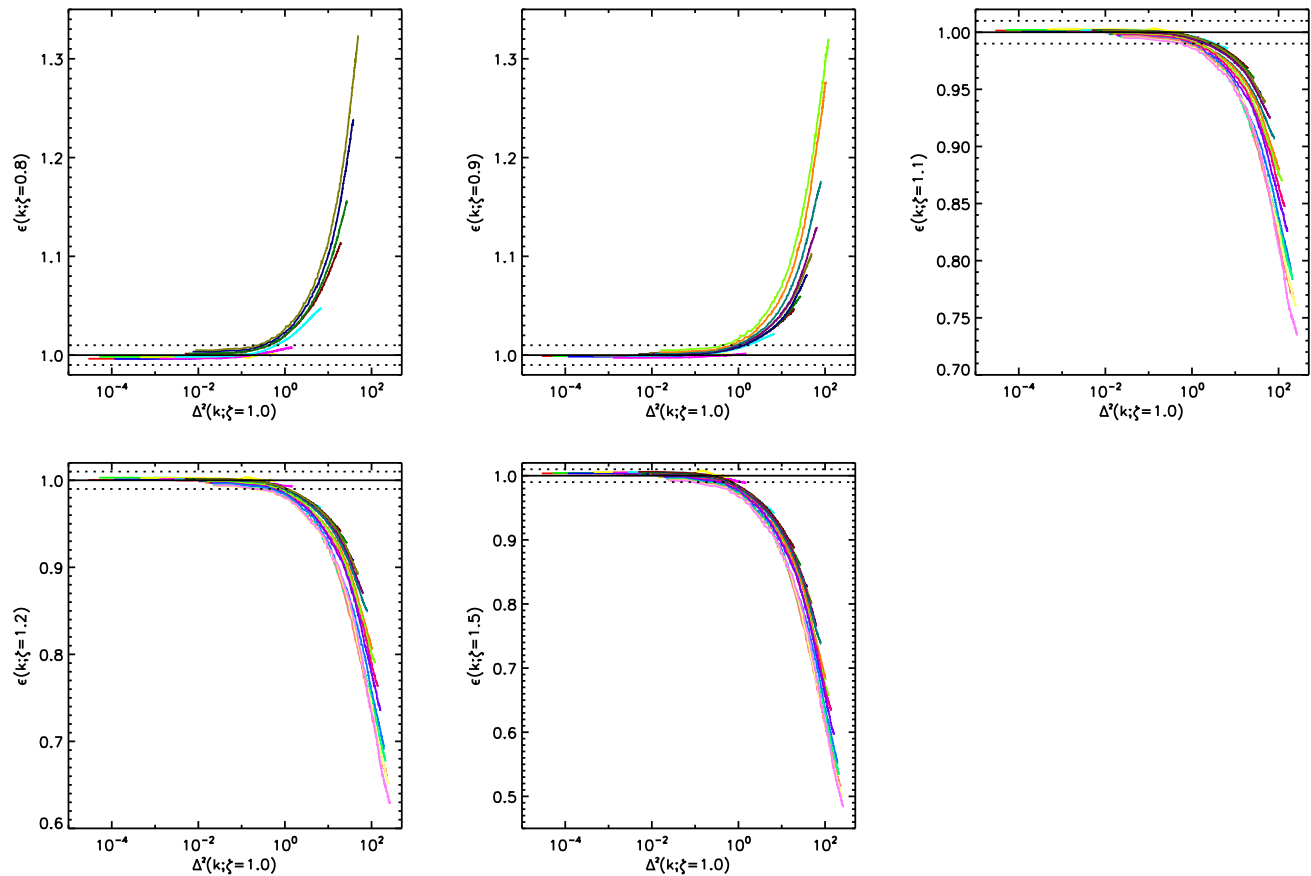


FIG. 4: The ratios of the nonlinear power spectra of MG models to the ones in Λ CDM when they have the same linear power. Results shown in different panels correspond to MG models of different ζ values. Different colors in each panel show different output redshifts. The ones that reach larger $\Delta^2(k, \zeta = 1)$ have lower redshifts. The two dotted black lines are in the 1% limit. In the bottom-right panel, we show the curves for ϵ of different values of ζ (shown in different line-styles). This comparison locates at the corresponding redshift with $z_s = 1.2$. [See the electronic edition of the Journal for a color version of this figure.]

IV. SIMULATION RESULTS

For the baseline — Λ CDM simulation, we choose 21 snapshots, whose redshift z_S is shown in Table I. We then run five MG simulations. We turn on the modified gravity at $z < z_{\text{MG}} = 100$. This is certainly not an unique choice, nor backed up by a solid argument. For example, we could turn on the modified gravity at a much later epoch. This will be the topic for future study. Naturally, ζ adopted in the simulations should cover the range allowed by present observations. Although there is no direct constraint for this particular type of MG in the literature, current constraints on MG (e.g. the parameterization investigated by [55], the gravitational slip parameter ϖ in [56] and η in [57]) imply that, the current constraint on ζ reaches no better than $\sim 10\%$ accuracy. This instructs us to adopt $\zeta = 0.8, 0.9, 1.1, 1.2$ for the simulations. We also run a simulation with $\zeta = 1.5$. Structure growth in the $\zeta = 1.5$ model is very likely too fast to fit existing observations (Fig. 3). Nevertheless, we include this simulation since dramatic modifications

in GR highlight signatures of MG in the nonlinear evolution, lead to better understanding of nonlinearity in MG models and help to improve the generality of fitting formulae based on these simulations [75].

The outputs of these simulations are chosen according to Eq. 3, such that the linear power spectrum of the given MG model at z_ζ is identical to that of Λ CDM at z_S . The corresponding z_ζ is shown in Table I. Since all simulations stop at $z = 0$ and linear density growth in $\zeta < 1$ universe is slower than that in Λ CDM (Fig. 3), there will be no available z_ζ for comparison in $\zeta < 1$ simulations.

The main simulation results are shown in Fig. 4. As a reminder, the function $\epsilon - 1$ is the relative difference between the nonlinear matter power spectrum in the MG model and the corresponding one in the standard Λ CDM [Eq. 5]. By design, it scales out the difference in the linear density growth rate and thus highlights other factors determining the nonlinear power spectrum. Furthermore, due to this particular design, we are able to reduce the possible numerical artifacts and model the nonlin-

earity to 1% accuracy. To better show the effect of non-linearity, we plot ϵ against the nonlinear matter power spectrum variance $\Delta^2(k; z_S, \zeta = 1)$. To illustrate the evolution of ϵ , we plot all ϵ of the same ζ in the same plot. At the bottom-right panel of Fig. 4, we show a comparison between different values of ζ . The redshifts for different ζ of this comparison are selected when they have the same linear power spectrum as Λ CDM simulation at $z_s = 1.20$.

A. Signatures of modified gravity in the nonlinear regime

The results in Fig. 4 shows significant imprints ($\epsilon \neq 1$) of modified gravity in the nonlinear evolution. Deviation of ϵ from unity becomes stronger at smaller scales and lower redshifts where nonlinearity is stronger. We find that, by proper scaling of Δ^2 , curves of Δ^2 - ϵ of fixed ζ can fall upon each other. We will discuss this behavior further in the Appendix and show its application to develop a fitting formula of ϵ , accurate to $\sim 1\%$. Whether or not this behavior is generic will be investigated in future studies.

There is another interesting behavior in the nonlinear evolution. The density growth in $\zeta > 1$ cosmology is faster (Fig. 3). However, after scaling out the linear growth, the normalized nonlinear evolution is actually slower (namely, $\epsilon < 1$ when $\zeta > 1$, Fig. 4). When $\zeta < 1$, the behavior is opposite ($\epsilon > 1$).

The halo model may explain such behavior. The nonlinear power spectrum can be decomposed into two terms [68]:

$$\Delta_{\text{NL}}^2(k, z) = \Delta_L^2(k, z) \left[\int_0^\infty M \delta(k|M, z) b(M) \frac{dn}{dM} dM \right]^2 + \frac{k^3}{2\pi^2} \int_0^\infty M^2 \delta^2(k|M, z) \frac{dn}{dM} dM. \quad (6)$$

Here, $\delta(k|M, z)$ is the Fourier transform of the density profile of a halo with mass M at redshift z , normalized so that $\delta(k \rightarrow 0) \rightarrow 1$. The halo abundance is dn/dM , and for convenience it is normalized such that $\int M dn = 1$. The first term on the right hand of the equation is the two-halo term, which dominates in the linear regime. The second term is the one-halo term, which dominates in the strongly nonlinear regime. Since $\delta(k \rightarrow 0) \rightarrow 1$ is independent of the halo density profile and $\int M b(M) dn = 1$, the two-halo term is not very sensitive to the halo density profile. Since $D(z_\zeta, \zeta) = D(z_S, \zeta = 1)$, as required, the two-halo term in the MG model is (roughly) equal to the two-halo term in Λ CDM, where they are dominant. On the other hand, in the nonlinear regime, the one-halo term strongly depends on the halo density profile, which depends on the structure growth history. Since structure grows faster in $\zeta > 1$ cosmology, we have $z_\zeta > z_S$. Halos in this universe form in a background with higher mean density ($\propto (1+z)^{-3}$). We then expect them to have a

smaller concentration [69]. For the same mass, a smaller concentration means a smaller $\delta(k|M, z)$ and a smaller contribution from the one-halo term. We then expect $\Delta_{\text{NL}}^2(k; z_\zeta, \zeta) < \Delta_{\text{NL}}^2(k; z_S, \zeta = 1)$ and thus $\epsilon(\zeta > 1) < 1$ in the nonlinear regime. We defer this investigation to a forthcoming paper, where we will measure and compare the halo mass functions and profiles between MG models and Λ CDM. For the same reason, we expect $\epsilon(\zeta < 1) > 1$ in the nonlinear regime. Whether or not the halo model will lead to a satisfying description of ϵ and thus the nonlinear power spectrum in MG models is an interesting project for further investigation.

In a word, large deviation of ϵ from unity implies that there is valuable information of gravity encoded in the nonlinear regime, which is complementary to those encoded in the linear matter power spectrum at the same epoch. It will be interesting to quantify how significantly this imprint of gravity in the nonlinear regime can improve cosmological tests of gravity,

B. Implications on the applicability of some existing fitting formulae

The particular definition of ϵ allows us to address a key question in understanding the nonlinearity, *is the nonlinear power spectrum uniquely determined by the linear one at the same epoch?* Equivalently, if the linear matter power spectra of two cosmologies are identical, will the corresponding nonlinear matter power spectra be identical?

The influential HKLM (Hamilton, Kumar, Lu and Matthews) procedure [58] assumes so. It postulates the existence of an one-to-one mapping between the linear correlation function at a linear scale and the nonlinear correlation function at the corresponding nonlinear scale. Reference [59] found that this mapping depends on the slope of the linear power spectrum. Hence after, the slope dependence has been explicitly incorporated in several fitting formulae, including the popular PD96 fitting formula [46] and the Smith et al. 2003 halofit formula [47]. In these fitting formulae, the mapping is expressed in Fourier space, of the functional form $\Delta_{\text{NL}}^2(k_{\text{NL}}, z) = \aleph(\Delta_L^2(k, z))$. This mapping is non-local. For example, in PD96, $\Delta_{\text{NL}}^2(k_{\text{NL}}, z)$ depends not only on $\Delta_L^2(k_L, z)$ at the corresponding linear scale k_L , but also on the effective power index n_{eff} at some linear scale, often chosen to be k_L or $k_L/2$. Furthermore, the mapping has extra dependences on cosmology. In PD96, $\Delta_{\text{NL}}^2(k_{\text{NL}}, z) = \aleph(\Delta_L^2(k, z), g(z))$. The cosmological dependence $g(z)$ has clear physical meaning, $g(z) \propto D(z)(1+z)$ and is normalized to $g(z \rightarrow \infty) = 1$. In the halofit, $\Delta_{\text{NL}}^2(k_{\text{NL}}, z) = \aleph(\Delta_L^2(k, z), \Omega_m)$, where Ω_m explicitly enters several fitting parameters. For a comprehensive review, refer to [47].

The HKLM procedure and its variations are successful in capturing the nonlinearities in CDM plus GR simulations. For this reason, they are often extended to predict

the nonlinear matter power spectrum in MG/dark energy models [57, 60–63]. The applicability of the resulting fitting formulae to MG models has been tested against several MG simulations [40, 64, 65]. In general, there is reasonable agreement at the $\sim 10\%$ level. But discrepancies are also noticed (e.g. [40, 65]). Our simulations, with improved simulation accuracy, improved power spectrum measurement method and specifically designed statistics, are able to identify the discrepancies at the 1% level.

Our simulation results (Fig. 4) show unambiguously that $\epsilon \neq 1$ in the nonlinear regime. For a 10% deviation from GR ($\zeta = 1.1$, or $\zeta = 0.9$), the resulting nonlinear power spectra can differ by 20%-30% at $\delta \sim 10$ ($\Delta^2 \sim 100$), to the corresponding one in the Λ CDM. The deviation becomes larger if the deviation of ζ from unity is larger. Quite obviously, the nonlinear matter power spectrum is not completely determined by the linear one at the same epoch. Reference [66] demonstrated by the case of dynamical dark energy, that the structure growth history is also responsible for shaping the nonlinear matter power spectrum. The MG models we investigate have a different structure growth history (e.g. different structure growth rate), and this may explain the observed significant deviation of ϵ from unity.

Our simulation set up allows us to evaluate the applicability of using several existing fitting formulae to MG models even without directly testing them. Since all the simulations have identical linear power spectra and the present day matter density Ω_m , the halofit would then predict $\epsilon = 1$. Our simulation result of ϵ then implies that a $\sim 20\%$ error may occur if one uses the halofit to calculate $\Delta_{\text{NL}}^2(\zeta = 1.1)$ (and $\Delta_{\text{NL}}^2(\zeta = 0.9)$) at the over density $\delta \sim 10$. The application of PD96 to MG models is a little bit tricky. In PD96, $g(z)$ is the ratio of the linear density growth rate between the given CDM cosmology and the $\Omega_m = 1$ flat universe. However, this form of $g(z)$, despite its clear physical meaning, does not apply to more general cases, such as the case of dynamical dark energy models [11]. Furthermore, PD96 is based on the stable clustering hypothesis. N-body simulations show that this hypothesis is problematic [47, 67]. Simple extrapolation of PD96 to the MG models should be avoided too.

V. DISCUSSION AND CONCLUSION

In this paper, we modify the GADGET-2 TreePM code to run a set of simulations for parameterized modified gravity models. As the first paper in a series, we focus on the nonlinear power spectrum in MG models. We take several steps to improve/test the model and simulation accuracy. First, we adopt an advanced analysis method to improve the power spectrum measurement. We then test the impact of various mass and force resolution, time step, initial redshift, and box size on the nonlinear power spectrum, and find suitable simulation specifications which meet our accuracy requirement. Fi-

nally, we focus on a particular quantity ϵ , the ratio between the nonlinear power spectra between MG models and Λ CDM with the same power spectra at a large linear scale. This quantity can be measured to higher accuracy than the nonlinear power spectrum itself, since much of the sample variance and simulation artifacts are reduced in ϵ . By construction, deviation of ϵ from unity is a signature of MG imprinted in the nonlinear evolution. It also means that the nonlinear matter power spectrum is not uniquely fixed by the linear one at the same redshift. It thus also represents the minimum systematical error induced by simply extrapolating some existing fitting formulae to these MG models. We find that, the deviation of ϵ from unity can reach $O(0.1)$ where the rms density fluctuation reaches 10, for MG models with a 10% deviation from GR. As an exercise toward a general fitting formula of this signature of MG, we develop a simple fitting formula of ϵ , accurate to $\sim 1\%$, working for the particular MG models that we investigate.

Significant improvements are required to reach precision modeling of the nonlinear matter power spectrum in more general MG models. In the next steps, we will run more simulations with larger box sizes, 1024^3 or more particles, various initial conditions, and various expansion histories.

More importantly, we need to explore larger MG parameter space. For example, we may need to vary z_{MG} to see its influence. Furthermore, instead of taking ζ as a step function with no scale dependence, we shall explore more complicated time dependent and scale dependent ζ models. In a companion paper, we will explore the minimalist MG model (γ -index, [33]), which has been adopted by the Figure of Merit Science Working Group (FoMSWG) [70] for forecasting. In this model, the linear density growth rate is given by $f(a) \equiv d \ln D(a) / d \ln a = \Omega_m^\gamma(a)$. Here, the growth index γ is a constant, whose value is $\simeq 0.55$ in Λ CDM. Stage-IV dark energy surveys can constrain this parameter with a rms error $O(0.01)$ (e.g. [71]). $\Omega_m(a) = \Omega_0 a^{-3} / (H^2 / H_0^2)$ is the matter density at redshift $z = 1/a - 1$. One particular advantage of this parameterization is that, since $\Omega_m(a \rightarrow 0) \rightarrow 1$, even for a model with time-constant γ can approach GR at high redshift.

The ζ parameterization can incorporate this model. The corresponding ζ can be obtained from Eq. 3,

$$\zeta = \frac{2f^2 + f(2 + H'a/H) + af'}{3\Omega_m(a)}, \quad ' \equiv \frac{d}{da}. \quad (7)$$

It is interesting to see whether new features will arise in the nonlinear regime and how to extend the proposed fitting scheme for this MG model.

Its is much harder to simulate realistic MG models such as $f(R)$ and DGP, which have complicated environmental dependences. We hope that, studies on MG models without environmental dependence can provide useful templates to understand these MG models.

Acknowledgments

We thank Volker Springel for the N-genic, public code GADGET-2 and detailed help. We thank Youcai Zhang, Raul Angulo, Klaus Dolag and Till Sawala for valuable discussions. This work is supported in part by the one-

hundred talents program of the Chinese academy of science, the national science foundation of China (grant No. 10533030, 10821302, 10925314 & 10973027), the CAS grant KJCX3-SYW-N2 and the 973 program grant No. 2007CB815401 & 2007CB815402.

-
- [1] E. Komatsu, et al., *ApJS*, 180, 330 (2009) [arXiv:0803.0547]
- [2] A. Albrecht et al., [arXiv:astro-ph/0609591]
- [3] B. Jain, P. Zhang, *Phys.Rev.D* 78, 063503 (2008) [arXiv:0709.2375]
- [4] K. Heitmann, P.M. Ricker, M.S. Warren, S. Habib, *ApJS*, 160, 28 (2005) [arXiv:astro-ph/0411795]
- [5] K. Heitmann, M. White, C. Wagner, S. Habib, D. Higdon, [arXiv:0812.1052]
- [6] K. Heitmann, et al., *Astrophys. J.*, 705, 156 (2009) [arXiv:0902.0429]
- [7] Earl Lawrence, Katrin Heitmann, Martin White, David Higdon, Christian Wagner, Salman Habib, Brian Williams, [arXiv:0912.4490]
- [8] P. McDonald, Hy Trac, C. Contaldi, *Mon.Not.Roy.Astron.Soc.*, 366, 547-556 (2006) [arXiv:astro-ph/0505565]
- [9] E.V. Linder, M. White, *Phys.Rev.D* 72, 061304 (2005) [astro-ph/0508401]
- [10] M.J. Francis, G.F. Lewis, E.V. Linder, *Mon.Not.Roy.Astron.Soc.* 380, 1079 (2007) [arXiv:0704.0312]
- [11] C. Ma, R.R. Caldwell, P. Bode, L. Wang, *Astrophys. J.*, 521, L1 (1999) [arXiv:astro-ph/9906174]
- [12] M. Baldi, V. Pettorino, G. Robbers, V. Springel, [arXiv:0812.3901]
- [13] M. Milgrom, *Astrophys. J.*, 270, 371 (1983); J.D. Bekenstein, *Phys.Rev.D* 70, 083509 (2004) [arXiv:astro-ph/0403694]
- [14] C. Skordis, D.F. Mota, P.G. Ferreira, C. Boehm, *Phys.Rev.Lett.* 96, 011301 (2006) [arXiv:astro-ph/0505519]; C. Skordis, *Phys.Rev.D* 74, 103513 (2006) [arXiv:astro-ph/0511591]; S. Dodelson, M. Liguori, *Phys.Rev.Lett.* 97, 231301 (2006) [arXiv:astro-ph/0608602]
- [15] G. Dvali, G. Gabadadze, M. Porrati, *Phys.Lett.B* 485, 208 (2000) [arXiv:hep-th/0005016]; C. Deffayet, *Phys.Lett.B*, 502, 199 (2001) [arXiv:hep-th/0010186]
- [16] A. Lue, R. Scoccimarro, G. Starkman, *Phys.Rev.D* 69, 124015 (2004) [arXiv:astro-ph/0401515]; K. Koyama, R. Maartens, *JCAP*, 0601, 016 (2006) [arXiv:astro-ph/0511634]
- [17] S.M. Carroll, V. Duvvuri, M. Trodden, M.S. Turner, *Phys.Rev.D* 70, 043528 (2004) [arXiv:astro-ph/0306438]; S.M. Carroll, A. De Felice, V. Duvvuri, D.A. Easson, M. Trodden, M.S. Turner, *Phys.Rev.D* 71, 063513 (2005) [arXiv:astro-ph/0410031]
- [18] P. Zhang, *Phys.Rev.D* 73, 123504 (2006) [arXiv:astro-ph/0511218]. The particular $f(R)$ model studied in this paper suffers instabilities in the structure formation. However, the derived linear perturbation equations at sub-horizon scales are correct. The key approximation in the derivation, namely the quasi-static approximation, adopted in this analysis, is later confirmed by, e.g. [20].
- [19] Y.S. Song, W. Hu, I. Sawicki, *Phys.Rev.D* 75, 044004 (2007) [astro-ph/0610532]
- [20] A. de la Cruz-Dombriz, A. Dobado, A. L. Maroto, *Phys.Rev.D* 77, 123515 (2008) [arXiv:0802.2999]
- [21] S. Nojiri, S. D. Odintsov, *Phys.Rev.D* 68, 123512 (2003) [hep-th/0307288]; S. Nojiri, S. D. Odintsov, [hep-th/0601213]
- [22] W. Hu, I. Sawicki, *Phys.Rev.D* 76, 104043 (2007) [arXiv:0708.1190]
- [23] K. Koyama, A. Taruya, T. Hiramatsu, *Phys.Rev.D* 79, 123512 (2009) [arXiv:0902.0618]
- [24] R. Scoccimarro, [arXiv:0906.4545]
- [25] G. Cognola et al, *Phys.Rev.D* 77, 046009 (2008) [arXiv:0712.4017]
- [26] H. Oyaizu, *Phys.Rev.D* 78, 123523 (2008) [arXiv:0807.2449]
- [27] F. Schmidt, M. Lima, H. Oyaizu, W. Hu, *Phys.Rev.D* 79, 083518 (2009) [arXiv:0812.0545]
- [28] H. Oyaizu, M. Lima, W. Hu, *Phys.Rev.D* 78, 123524 (2008) [arXiv:0807.2462]
- [29] G. Cognola et al, *Phys.Rev.D* 79, 044001 (2009) [arXiv:0810.4989]
- [30] F. Schmidt, *Phys.Rev.D* 80, 043001 (2009) [arXiv:0905.0858]; K.C. Chan, R. Scoccimarro, [arXiv:0906.4548]
- [31] Baojiu Li, Hongsheng Zhao. *Phys.Rev.D* 80, 064007 (2009) [arXiv:0906.3880]; HongSheng Zhao, Andrea Macciò, Baojiu Li, Henk Hoekstra, Martin Feix, [arXiv:0910.3207]; Baojiu Li, Hongsheng Zhao, [arXiv:1001.3152]
- [32] E.V. Linder, *Phys.Rev.D* 72, 043529 (2005) [arXiv:astro-ph/0507263]
- [33] D. Huterer, E.V. Linder, *Phys.Rev.D* 75, 023519 (2007) [astro-ph/0608681]
- [34] J.P. Uzan, *Gen.Rel.Grav.* 39, 307-342 (2007) [arXiv:astro-ph/0605313]
- [35] R. Caldwell, A. Cooray, A. Melchiorri, *Phys.Rev.D* 76, 023507 (2007) [arXiv:astro-ph/0703375]
- [36] P. Zhang, M. Liguori, R. Bean, S. Dodelson, *Phys.Rev.Lett.* 99, 141302 (2007) [arXiv:0704.1932]
- [37] L. Amendola, M. Kunz, D. Sapone, *JCAP* 0804, 013 (2008) [arXiv:0704.2421]
- [38] Constantinos Skordis. *Phys.Rev.D* 79, 123527 (2009) [arXiv:0806.1238]
- [39] A. Shirata, Y. Suto, C. Hikage, T. Shiromizu, N. Yoshida, *Phys.Rev.D* 76, 044026 (2007) [arXiv:0705.1311]; M.C. Martino, H.F. Stabenau, R.K. Sheth, *Phys.Rev.D* 79, 084013 (2009) [arXiv:0812.0200]
- [40] H.F. Stabenau, B. Jain, *Phys.Rev.D* 74, 084007 (2006) [arXiv:astro-ph/0604038];
- [41] P. Zhang, R. Bean, M. Liguori, S. Dodelson,

- [arXiv:0809.2836]
- [42] G.B. Zhao, L. Pogosian, A. Silvestri, J. Zylberberg, Phys.Rev.D 79, 083513 (2009) [arXiv:0809.3791]; G.B. Zhao, L. Pogosian, A. Silvestri, J. Zylberberg, [arXiv:0905.1326]
- [43] J. Guzik, B. Jain, M. Takada, [arXiv:0906.2221]
- [44] J. Khoury and A. Weltman, Phys. Rev. D 69, 044026 (2004) [arXiv:astro-ph/0309411]; J. A. R. Cembranos, Phys. Rev. D 73, 064029 (2006) [arXiv:gr-qc/0507039]; I. Navarro and K. Van Acoleyen, JCAP 0702, 022 (2007) [arXiv:gr-qc/0611127]; T. Faulkner, M. Tegmark, E. F. Bunn, and Y. Mao, Phys. Rev. D 76, 063505 (2007) [astro-ph/0612569]; W. Hu and I. Sawicki, Phys. Rev. D 76, 064004 (2007) [arXiv:0705.1158]
- [45] A. I. Vainshtein, Phys. Lett. B 39, 393 (1972); C. Defayet, G. Dvali, G. Gabadadze, and A. I. Vainshtein, Phys. Rev. D 65, 044026 (2002)
- [46] J.A. Peacock, S.J. Dodds, MNRAS, 280, 19 (1996) [arXiv:astro-ph/9603031]
- [47] R.E. Smith, et al., MNRAS, 341, 1311 (2003) [arXiv:astro-ph/0207664]
- [48] Emma Beynon, David J. Bacon, Kazuya Koyama, [arXiv:0910.1480]
- [49] V. Springel, N. Yoshida, S.D.M. White, New Astronomy, 6, 79 (2001) [arXiv:astro-ph/0003162]
- [50] V. Springel, MNRAS, 364, 1105 (2005) [arXiv:astro-ph/0505010]
- [51] Y.P. Jing, Astrophys. J. , 620, 559 (2005) [arXiv:astro-ph/0409240]
- [52] W. Cui, L. Liu, X. Yang, W. Yu, L. Feng, V. Springel, Astrophys. J. , 687, 738 (2008) [arXiv:0804.0070]
- [53] E. Sirko, Astrophys. J. , 634, 728 (2005) [arXiv:astro-ph/0503106]
- [54] Y.B. Zel'dovich, Astron. Astrophys., 5, 84 (1970)
- [55] Tomi Koivisto, David F. Mota, Phys.Rev.D 73, 083502 (2006) [astro-ph/0512135]
- [56] Scott F. Daniel, Robert R. Caldwell, Asantha Cooray, Alessandro Melchiorri, Phys.Rev.D 77, 103513 (2008) [arXiv:0802.1068]; Scott F. Daniel, Robert R. Caldwell, Asantha Cooray, Paolo Serra, Alessandro Melchiorri, Phys.Rev.D 80, 023532 (2009) [arXiv:0901.0919]
- [57] R. Bean, [arXiv:0909.3853v2]
- [58] A.J.S. Hamilton, P. Kumar, E. Lu, A. Matthews, Astrophys. J. , 374, L1-L4 (1991)
- [59] B. Jain, H.J. Mo, S.D.M. White, MNRAS, 276, L25 (1995) [arXiv:astro-ph/9501047]
- [60] L. Knox, Y.-S. Song J.A. Tyson, [arXiv:astro-ph/0503644]
- [61] Mustapha Ishak, Amol Upadhye and David N. Spergel. Phys.Rev.D 74, 043513 (2006) [arXiv:astro-ph/0507184]
- [62] Sheng Wang, Lam Hui, Morgan May and Zoltan Haiman. Phys.Rev.D 76, 063503 (2007) [arXiv:0705.0165]
- [63] O. Dore, et al., [arXiv:0712.1599v1]
- [64] I. Laszlo, R. Bean, Phys.Rev.D 77, 4048 (2008) [arXiv:0709.0307]
- [65] J. Khoury, M. Wyman, Phys.Rev.D 80, 4023 (2009) [arXiv:0903.1292]
- [66] Z.M. Ma, Astrophys. J. , 665, 887 (2007) [arXiv:astro-ph/0610213]
- [67] Y.P. Jing, Astrophys. J. , 550, L125 (2001) [arXiv:astro-ph/0101210]
- [68] Y.P. Jing, H.J. Mo, G. Boerner, Astrophysical Journal v494, p1 (1998); A. Cooray, R. Sheth, Phys.Rept., 372, 1 (2002) [arXiv:astro-ph/0206508]
- [69] D.H. Zhao, Y.P. Jing, H.J. Mo, G. Boerner, [arXiv:0811.0828]; D.H. Zhao, Y.P. Jing, H.J. Mo, G. Boerner, Astrophys. J. , 597, L9 (2003) [arXiv:astro-ph/0309375]
- [70] A. Albrecht, et al., [arXiv:0901.0721]
- [71] Arthur Stril, Robert N. Cahn, Eric V. Linder, [arXiv:0910.1833]
- [72] ζ defined here is equivalent to ζ in [3], up to a constant factor of $4\pi G$.
- [73] However, this does not mean that ζ and the expansion rate uniquely fix the gravitational lensing statistics, since gravitational lensing is determined by the combination $\phi - \psi \propto G_{\text{eff}}(1 + 1/\eta)\rho = \zeta\rho(1 + \eta)$. Since this relation is algebraic, there is no extra simulations required to evaluate the lensing statistics. The above arguments hold as long as $G_{\text{eff}}(k, z)$ and $\eta(k, z)$ are deterministic functions of scale k and redshift z .
- [74] This is not an arbitrary choice, as it appears to be. In general dark energy cosmology and MG cosmology, the expansion history and the structure formation are independent. Since the structure formation is affected by quantities such as the dark energy sound speed, the anisotropic stress, G_{eff} and η (and ζ) at sub-horizon scales do not affect the expansion. It is thus natural to fix the expansion rate matching the observations today and explore the possible difference in the structure growth.
- [75] We also run a simulation with $\zeta = 0.5$. We find that the structure growth in this model is too linear to be interesting.

Appendix A: The fitting formula

We demonstrate the feasibility to develop an accurate fitting formula for ϵ , which quantifies the difference of the nonlinear evolution between the MG cosmology and Λ CDM. In combination with the existing Λ CDM fitting formulae, the nonlinear power spectrum in MG models can be predicted. We only use the results of $\zeta > 1$ simulations to develop the fitting formula. We reserve the $\zeta < 1$ simulations to check the generality of our fitting formula. This fitting formula is by no mean applicable to general MG models. Nonetheless, we hope that it serves as an useful exercise toward more general fitting formula, which we will explore elsewhere.

1. Developing the fitting formula

As shown in Fig. 4, ϵ is a function of the scale, redshift and ζ ,

$$\begin{aligned} \epsilon(k, z_\zeta, \zeta) &= u(x, z_S, \zeta) \\ x &\equiv \Delta_{\text{NL}}^2(k, z_S, \zeta = 1). \end{aligned} \quad (\text{A1})$$

We will develop the fitting formula according to the following steps.

Step 1: By visually inspecting Fig. 4 for each ζ , it looks feasible to move each lines horizontally such that they fall upon each other. This horizontal shift indeed

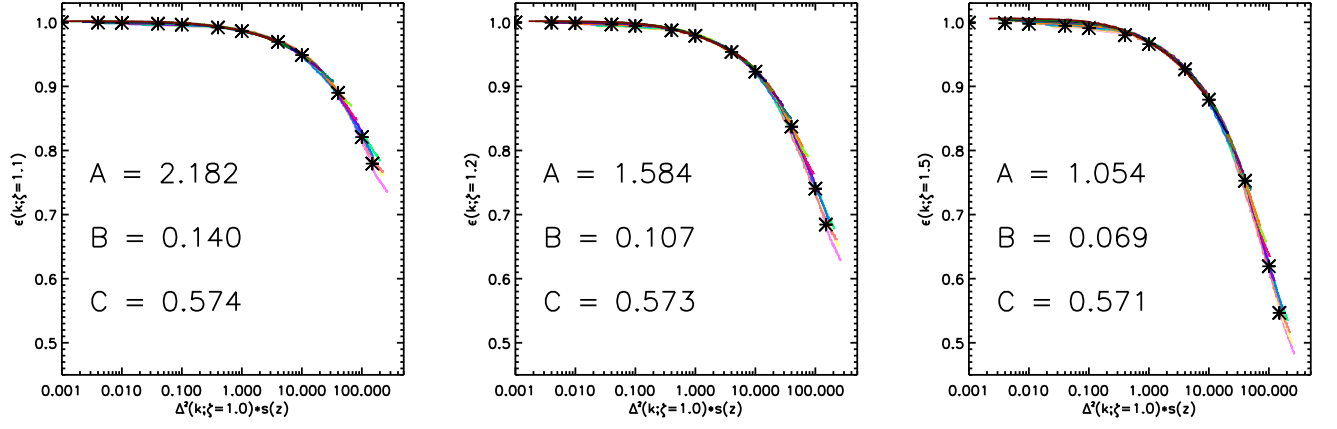


FIG. 5: Similar to Fig. 4, but only shown for results with $\zeta > 1$. In addition, lines corresponding to different redshifts are shifted by a factor of $s(z)$ as described in Eq. A3. These lines are then fitted with three parameters A , B and C . The asterisks are the fitting points produced by the fitting recipe.

works (Fig. 5). Mathematically, this means that we can find a shift function $s(z_S, \zeta)$, such that

$$u(x, z_S, \zeta) = u(y, \zeta); \quad y = x \times s(z_S, \zeta). \quad (\text{A2})$$

In the exercise, we fix ζ first. Then for each z_S (or the corresponding z_ζ), we find the suitable s , such that the corresponding curve, after the horizontal shift, overlaps with the one with $z_S = 0$. To do so, we have required that $s(z_S = 0, \zeta) = 1$. We find that higher redshift curves should be shifted more leftward. This requires that (i) $s(z_S)$ is positive, and (ii) $s(z_S)$ monotone decreases with respect to z_S . These requirements help us to find the following fitting function for s :

$$s(z_S, \zeta) = \left[\frac{D(z_S, \zeta = 1)}{D(z_S = 0, \zeta = 1)} \right]^{A(\zeta)}, \quad (\text{A3})$$

where $A(\zeta) > 0$.

Step 2: The next step is to figure out a suitable form for $u(y, \zeta)$, namely, to fit those curves in Fig. 5. There are several guidelines. (1) $u > 0$, since both power spectra must be positive. (2) $u(y, \zeta = 1) = 1$, by the definition. (3) $\epsilon = u < 1$ when $\zeta > 1$ and $\epsilon > 1$ when $\zeta < 1$ (Fig. 4). These behaviors motivate us to propose the following fitting function:

$$u(y, \zeta) = e^{(1-\zeta)B(\zeta)y^{C(\zeta)}}. \quad (\text{A4})$$

As long as $B(\zeta) > 0$, all three conditions are satisfied.

Step 3: For each ζ , we fit the simulation data and find the best fit A , B and C , whose values are shown in Fig. 5. We then need to find the suitable form to model the ζ dependence of these parameters. The following functions with the associated parameters provide a good fit:

$$\begin{aligned} A(\zeta) &= e^{(a_0 - \zeta)}, \quad a_0 = 1.745, \\ B(\zeta) &= b_0 + b_1 \zeta^{-4}, \quad b_{0,1} = 0.0429, 0.133, \\ C(\zeta) &= 0.573. \end{aligned} \quad (\text{A5})$$

2. Calculating the nonlinear power spectrum in MG models

We summarize the procedure to calculate the nonlinear matter power spectrum $\Delta_{\text{NL}}^2(k, z_\zeta, \zeta)$ using our fitting formula.

- For the given redshift z_ζ in the MG model, find the corresponding z_S in Λ CDM through Eq. 4. The two corresponding power spectra at large linear scale are then identical.
- Calculate $\Delta_{\text{NL}}^2(k, z_S, \zeta = 1)$. This can be done by using either direct Λ CDM simulations (as in our case) or existing fitting formulae such as the halofit.
- Combining Eqs. A2, A3, A4 & A5, we are then able to predict $\epsilon(k, z_\zeta, \zeta)$. In combination with $\Delta_{\text{NL}}^2(k, z_S, \zeta = 1)$, we can then predict the nonlinear matter power spectrum $\Delta_{\text{NL}}^2(k, z_\zeta, \zeta)$ in the given MG model.

3. Testing the fitting formula

Because of the very limited simulations that we have, we are not able to perform comprehensive tests against the generality of the fitting formulae. However, we are indeed able to check it against our $\zeta < 1$ simulations. Since we do not use these simulations to find the fitting parameters, these $\zeta < 1$ simulations can provide an independent check against our fitting formula.

In Fig. 6, we show the performance of our fitting formula. The ratios between the simulated and predicted nonlinear power spectrum of MG models are shown using different line styles for different ζ and redshifts as indicated. In general, our fitting formula is accurate to 1-2% in the range $k < 3h/\text{Mpc}$. Although results for the cases

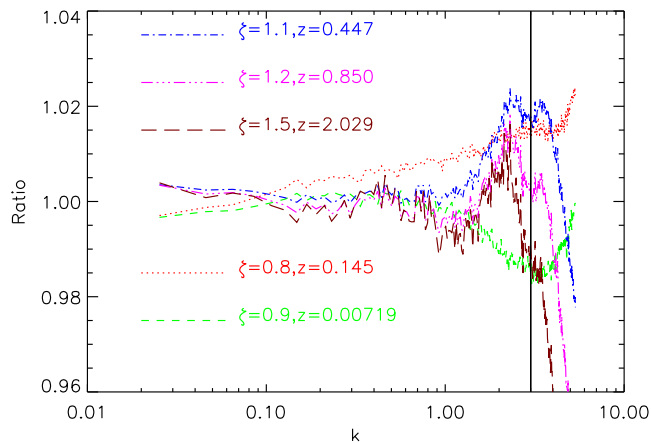


FIG. 6: Testing the accuracy of the fitting formula. We plot the power spectrum ratios as a function of k between the simulation results and our model predictions. Different ζ with its checking redshift are shown in different colors and line styles. The vertical line is at $k = 3 h\text{Mpc}^{-1}$, below which our simulation results are reliable, as shown in Sec. III.

with $\zeta < 1$ are extrapolations of our fitting formula, their performances are as good as for the $\zeta > 1$ cases. Such good performance demonstrates the applicability of our fitting formula. And we do not try to seek for possible slightly more accurate but much more complicated fitting formulae.

We have shown that the proposed fitting formula provides a good description of the nonlinear matter power spectrum, for the specific form of MG that we adopt. Is it applicable to other cases? We are not able to answer this question by the existing simulations. However, we still want to discuss a less general question, is it applicable to the MG models with $z_{\text{MG}} \neq 100$? In the fitting formula, the only quantity dependent of z_{MG} is $D(z_S, \zeta = 1) = D(z_\zeta, \zeta)$. This dependence alone may not be sufficient. It is very likely that A , B , and C depend on z_{MG} , too. This is a key issue for future investigation. Nevertheless, we show that it is possible to develop a fitting formula for MG models by the above simple technique. It may also be applicable to more general MG models. This is again an interesting issue for further investigation.